

Effects of gold nanorods modified with anti-epidermal growth factor receptor monoclonal antibody on laryngeal cancer cells

Fangzhou LIU¹†, Yan ZHU²†, Yichuan QIAN¹, Yanbin ZHAO¹, Xiaotong ZHAO¹, Jia ZHANG³, Yu ZHANG^{4*}, Yuan ZHANG¹

¹Department of Head and Neck Surgery, Jiangsu Cancer Hospital Affiliated to Nanjing Medical University, Nanjing, P. R. China

²Department of Pathology, The First Affiliated Hospital of Nanjing Medical University, Nanjing, P. R. China

³PET-CT Department, Jiangsu Cancer Hospital Affiliated to Nanjing Medical University, Nanjing, P. R. China

⁴School of Biological Sciences and Medical Engineering, Southeast University, Nanjing, P. R. China

Received: 31.08.2017 • Accepted/Published Online: 14.11.2017 • Final Version: 27.04.2018

Abstract: We aimed to evaluate the photothermal effects of gold nanorods (GNRs) modified with anti-epidermal growth factor receptor (EGFR) monoclonal antibody (mAb) on laryngeal cancer cells. EGFR protein expressions in HEP-2 cells, and normal laryngeal epithelial and laryngeal cancer tissues were detected by western blot. The cytotoxicity against HEP-2 and BEAS-2B cells was tested by MTT assay, and the photothermal effects were assessed by near-infrared (NIR) irradiation. The apoptosis of HEP-2 cells was detected by flow cytometry. EGFR expression in laryngeal cancer tissues was significantly higher than that in normal tissues ($P < 0.05$). The inhibitory effects of GNRs and anti-EGFR mAb/GNRs on the apoptosis of HEP-2 and BEAS-2B cells were enhanced with increasing dose. Anti-EGFR mAb/GNRs were more cytotoxic to HEP-2 cells and less cytotoxic to BEAS-2B cells than GNRs. NIR irradiation inhibited cell proliferation, which was enhanced with rising power, accompanied by continuously dropping survival rate. The apoptosis rate of the anti-EGFR mAb/GNRs group was significantly higher than that of the GNRs group, and the apoptosis rate of the irradiation + anti-EGFR mAb/GNRs group also significantly exceeded that of the irradiation + GNRs group ($P < 0.05$). Anti-EGFR mAb/GNRs promoted HEP-2 cell apoptosis more evidently than GNRs did. Functional modification of GNRs augmented the targeted specificity to cancer cells, biocompatibility, and stability. Anti-EGFR mAb/GNRs have great potential in biomedical fields.

Key words: Gold nanorod, epidermal growth factor receptor, monoclonal antibody, laryngeal cancer

1. Introduction

Laryngeal cancer is one of the most common malignant tumors of otolaryngology–head and neck surgery, and 93%–99% of all cases are diagnosed as squamous cell carcinoma. The 5-year survival rate of patients has been increased due to greatly improved surgery, radiotherapy, and chemotherapy. However, surgery easily leads to disability by severely damaging the laryngeal function, radiotherapy only works for early laryngeal cancer, and chemotherapy has intolerable toxic side effects (Misono et al., 2014; Haapaniemi et al., 2016; Wolf et al., 2017; Zahoor et al., 2017). Therefore, researchers have endeavored to find new therapies for the treatment of laryngeal cancer.

Gold nanorods (GNRs) are rod-like shaped plasmonic nanoparticles. As the most studied anisotropic gold nanoparticles, GNRs have been widely applied in biomolecular detection, medical imaging, disease treatment, and drug delivery. Near-infrared (NIR)

wavelengths are the “optical window” for biological tissues and so GNRs probes help NIR light to penetrate subcutaneous deep tissues for imaging and photothermal therapy. Most laser therapies depend on endoscope and fiber-optic bundles to transmit light into tumor tissues and to function selectively through intravenous injection of photosensitizers. Metals, especially gold nanoparticles, can be easily modified as ideal candidates for targeted therapy.

Particularly, antibody-based therapies are efficient and specific. Epidermal growth factor receptor (EGFR), which is a polypeptide chain consisting of 1186 amino acid residues, has tyrosine protein kinase activity and is widely distributed on the surfaces of most normal cells. Currently, high EGFR expressions have been detected in various tumor tissues, especially in head and neck squamous cell carcinoma (detection rate: 98.3%). Anti-EGFR monoclonal antibody (anti-EGFR mAb) is specifically localized on

† The two authors contributed equally to this study.

* Correspondence: zhangyu_seu@yahoo.com

oral squamous cell carcinoma and cervical cancer cells overexpressing EGFR (Zhong et al., 2013; Suman et al., 2014).

In the present study, laryngeal cancer cells (HEP-2) and lung normal epithelial cells (BEAS-2B) treated with GNRs were irradiated by NIR light at different powers, aiming to evaluate the targeted inhibitory effects of anti-EGFR mAb/GNRs. The findings provide reliable evidence for future targeted therapy of laryngeal cancer.

2. Materials and methods

2.1. Cell lines, tissues, and reagents

HEP-2 and BEAS-2B cells were purchased from the American Type Culture Collection (USA). After approval by the ethics committee of our hospital, laryngeal epithelial tissues and laryngeal squamous epithelial carcinoma tissues were collected from patients. GNRs and anti-EGFR mAb/GNRs were provided by the National Center for Nanoscience and Technology (China). Goat anti-mouse AP secondary antibody and β -actin mouse monoclonal antibody were bought from Sigma (USA). RPMI 1640, DMEM, penicillin, streptomycin, fetal bovine serum, and MTT were obtained from HyClone (USA).

2.2. Cell resuscitation and culture

A tube of cryo-preserved cells was taken out of a liquid nitrogen container, rapidly immersed in a 37 °C water bath, and shaken for 1–2 min using tweezers. Then 10 mL of complete culture medium was added to a culture dish, into which the cells were added, gently pipetted until uniformity was achieved, cultured in a 37 °C incubator containing 5% CO₂, digested with 0.25% trypsin when the adherence rate reached 80%, and passaged.

2.3. Western blot

Cells were digested, collected by centrifugation, resuspended by adding RIPA (50 mM pH 7.5 Tris-HCl, 150 mM NaCl, 1% NP-40, 0.5% sodium deoxycholate, 0.1% SDS), ultrasonicated, and centrifuged at 12000 rpm and 4 °C for 10 min. Each sample (50 μ g) was subjected to SDS-PAGE and electronically transferred to a nitrocellulose membrane that was then blocked in 5% skimmed milk at room temperature for 1 h, incubated overnight with primary antibody at 4 °C, washed, incubated with secondary antibody at 37 °C for 1 h, developed by ECL reagent, and scanned. Relative protein expression level was corrected by internal reference and analyzed by Quantity-One.

2.4. Detection of cytotoxicity of GNRs and anti-EGFR mAb/GNRs by MTT assay

Cells in the logarithmic growth phase were collected, added to 96-well culture plates at the density of 10⁴/well (100 μ L each well), and incubated at 37 °C in a 5% CO₂ atmosphere. After cell adherence, GNRs and anti-EGFR

mAb/GNRs solutions at the final concentrations of 0.01, 0.02, 0.04, 0.08, 0.16, and 0.32 nM were added (100 μ L each well). Each concentration was tested in triplicate. PBS was used as a negative control. Subsequently, the cells were incubated at 37 °C in a 5% CO₂ atmosphere for 16–48 h, observed under an inverted microscope, washed carefully two or three times with PBS, and incubated with MTT solution (20 μ L each well, 5 mg/mL, i.e. 0.5% MTT) for another 4 h. The culture medium was then carefully sucked out. Afterwards, 150 μ L of DMSO was added to each well, and the culture plate was shaken at low speed for 10 min to completely dissolve crystals. The absorbance of each well was detected at 595 nm by a microplate reader. Cell viability = $\text{OD}_{\text{experimental group}} / \text{OD}_{\text{negative control}} \times 100\%$.

2.5. Detection of cell viability after NIR photothermal therapy by MTT assay

Cells (HEP-2 or BEAS-2B) in the logarithmic growth phase were collected, added to 96-well culture plates at the density of 10⁴/well (100 μ L each well), and incubated at 37 °C in a 5% CO₂ atmosphere. Then the cells were divided into an irradiation group, a 0.04 nM GNRs group, and a 0.04 nM anti-EGFR mAb/GNRs group. Each concentration was tested in triplicate. For the three groups, 450 μ L of fresh culture medium, 450 μ L of 0.04 nM GNRs solution, and 450 μ L of 0.04 nM anti-EGFR mAb/GNRs solution were added consecutively, and the cells were cultured for 8 h. Irradiation conditions: Irradiation by NIR light (0.8–4 w/cm²) at 808 nm for 5 min, culture for 24 h, and incubation with MTT solution (20 μ L each well, 5 mg/mL, i.e. 0.5% MTT) for another 4 h. The culture medium was then carefully sucked out. Afterwards, 150 μ L of DMSO was added to each well, and the culture plate was shaken at low speed for 10 min to completely dissolve the crystals. The absorbance of each well was detected at 595 nm by a microplate reader. Cell viability = $\text{OD}_{\text{experimental group}} / \text{OD}_{\text{negative control}} \times 100\%$.

2.6. Detection of cell apoptosis after NIR photothermal therapy by flow cytometry

HEP-2 cells in the logarithmic growth phase were collected, added into 96-well culture plates at the density of 10⁴/well (100 μ L each well), and incubated at 37 °C in a 5% CO₂ atmosphere. Then the cells were divided into an irradiation group, a 0.04 nM GNRs group, a 0.04 nM anti-EGFR mAb/GNRs group, a 0.04 nM GNRs + irradiation group, and a 0.04 nM anti-EGFR mAb/GNRs + irradiation group. Each concentration was tested in triplicate. For the irradiation group, 450 μ L of fresh culture medium was added, and 450 μ L of GNRs or anti-EGFR mAb/GNRs solution was added to the other groups. The cells were thereafter cultured for 8 h. Irradiation conditions: Irradiation by NIR light (2.4 w/cm²) at 808 nm for 5 min. Subsequently, the adherent cells were digested by trypsin, and the suspending cells were collected. After the culture medium was discarded,

the cells were suspended by adding PBS, gently mixed with 10 μ L of annexin V-FITC and 10 μ L pf PT, incubated at room temperature in the dark for 20 min, and detected by flow cytometry.

2.7. Statistical analysis

Each experiment was independently performed in triplicate. All data were analyzed by SPSS 22.0, and the results were expressed as mean \pm standard deviation. Comparisons between two groups were conducted by the t test, and those among multiple groups were carried out by one-way analysis of variance. $P < 0.05$ was considered statistically significant.

3. Results

3.1. EGFR expressions in HEP-2 cells, laryngeal cancer tissues, paracancerous tissues, and normal control tissues detected by western blot

Western blot showed that EGFR expressions in HEP-2 cells and laryngeal cancer tissues were significantly higher than those in paracancerous and normal control tissues ($P < 0.05$) (Figure 1).

3.2. Cytotoxicities of GNRs and anti-EGFR mAb/GNRs detected by MTT assay

The MTT assay showed that the inhibitory effects of GNRs and anti-EGFR mAb/GNRs on the viability of HEP-2 and

BEAS-2B cells were enhanced with increasing dose. Anti-EGFR mAb/GNRs were more cytotoxic to HEP-2 cells and less cytotoxic to BEAS-2B cells than GNRs (Figure 2).

3.3. Cell survival rates after NIR irradiation detected by MTT assay

As exhibited in Figures 3 and 4, NIR irradiation inhibits cell proliferation, which is enhanced by rising irradiation power, accompanied by continuously dropping survival rate. For HEP-2 cells, the irradiation, GNRs, and anti-EGFR mAb/GNRs groups had significantly different survival rates ($P < 0.05$), and the rate of the anti-EGFR mAb/GNRs group was significantly lower than that of the GNRs group ($P < 0.05$). For BEAS-2B cells, the three groups had similar survival rates ($P > 0.05$) at the irradiation power of ≤ 2.4 w/cm². The survival rates of the GNRs and anti-EGFR mAb/GNRs groups were significantly lower than that of the irradiation group at 3.2 and 4.0 w/cm² ($P < 0.05$), but the first two groups had similar results ($P > 0.05$).

3.4. Cell apoptosis after NIR irradiation detected by flow cytometry

Flow cytometry exhibited that the apoptosis rate of the anti-EGFR mAb/GNRs group was significantly higher than that of the GNRs group, and the apoptosis rate of the irradiation + anti-EGFR mAb/GNRs group also significantly exceeded that of the irradiation + GNRs

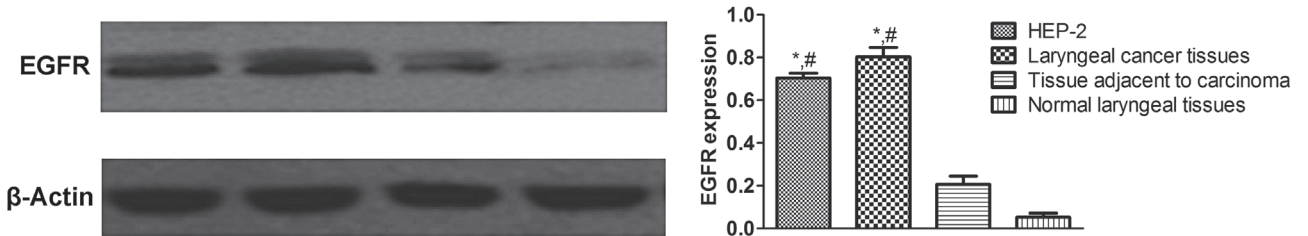


Figure 1. EGFR expressions detected by western blot. *Compared with paracancerous tissues, $P < 0.05$; #compared with normal tissues, $P < 0.05$.

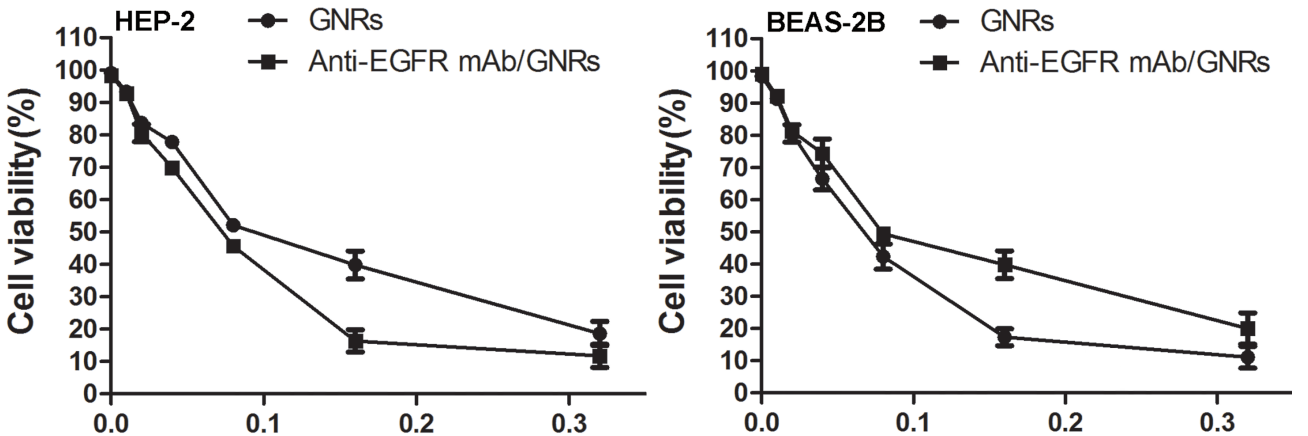


Figure 2. Cytotoxicities of GNRs and anti-EGFR mAb/GNRs detected by MTT assay.

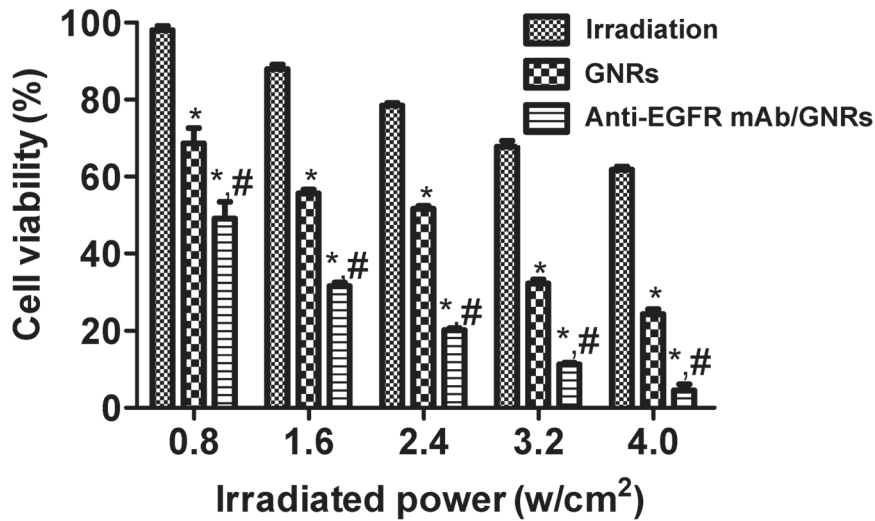


Figure 3. HEP-2 cell survival rates after NIR irradiation detected by MTT assay. *Compared with irradiation group, $P < 0.05$; compared with GNRs group, $P < 0.05$.

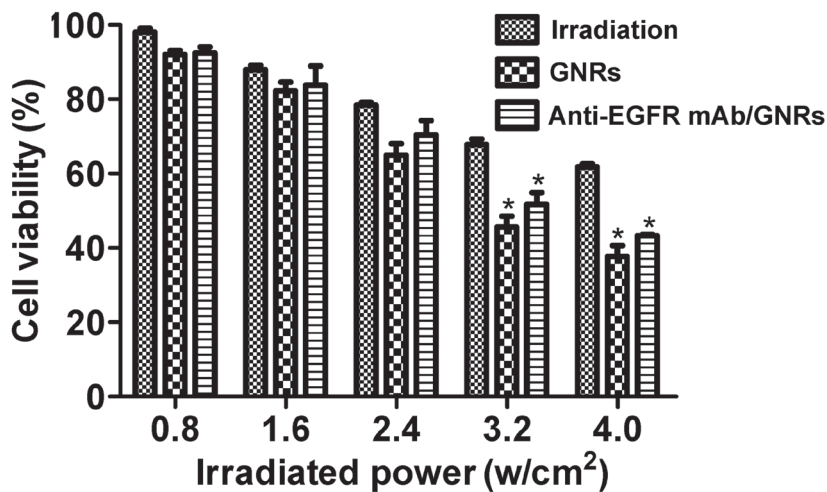


Figure 4. BEAS-2B cell survival rates after NIR irradiation detected by MTT assay. *Compared with irradiation group, $P < 0.05$.

group ($P < 0.05$) (Figure 5). Thus, anti-EGFR mAb/GNRs promoted HEP-2 cell apoptosis more evidently than GNRs did.

3.5. Cleaved PARP and cleaved caspase-3 expressions detected by western blot

The anti-EGFR mAb/GNRs group had significantly higher expressions of cleaved PARP and caspase-3 than those of the GNRs group, and the expressions of the irradiation + anti-EGFR mAb/GNRs group also significantly exceeded those of the irradiation + GNRs group ($P < 0.05$) (Figure 6). Hence, GNRs facilitated cell proliferation and apoptosis mainly by promoting the expressions of apoptosis-related proteins, further verifying that anti-EGFR mAb/GNRs

promoted HEP-2 cell apoptosis more effectively than GNRs did.

4. Discussion

EGFR is the first discovered cancer-related cell surface receptor. Discovering the active form of EGFR proto-oncogene encoding EGFR kinase established the relationship between this proto-oncogene and cancer. For over 20 years afterwards, abnormal regulation of EGFR receptor has been closely related to the formation of a variety of human cancers. High expressions of EGFR have been detected in various types of tumors such as colorectal cancer, breast cancer, pancreatic cancer,

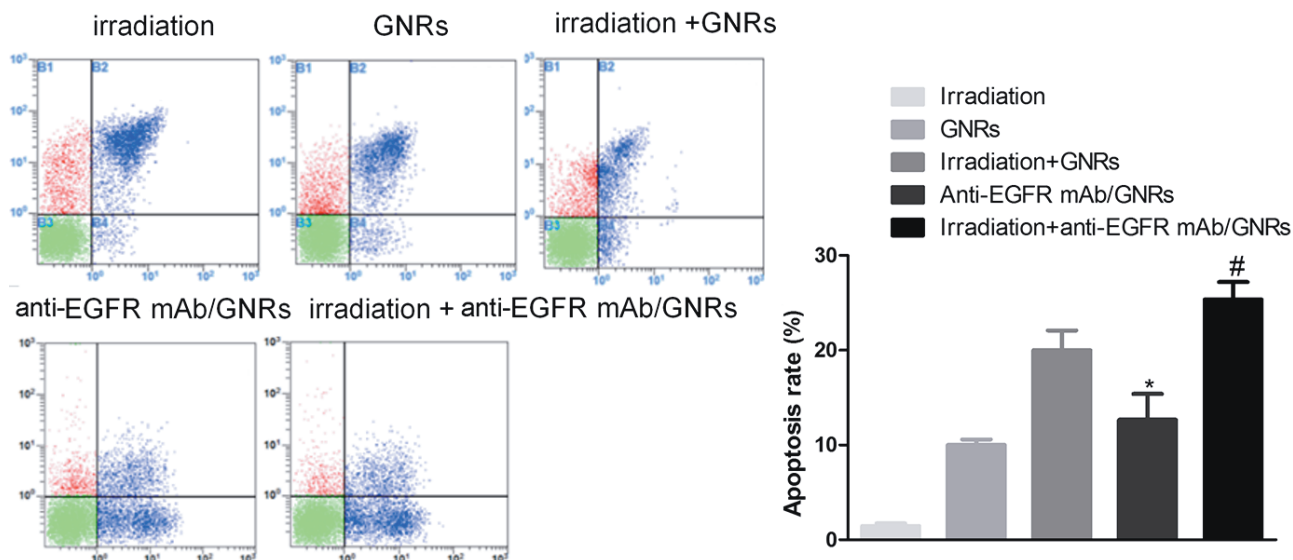


Figure 5. HEP-2 cell apoptosis after NIR irradiation detected by flow cytometry. *Comparison between anti-EGFR mAb/GNRs group and GNRs group, $P < 0.05$; #comparison between irradiation + anti-EGFR mAb/GNRs group and irradiation + GNRs group, $P < 0.05$.

prostate cancer, and nonsmall cell lung cancer, and the detection rate reaches up to 98.3% in head and neck squamous cell carcinoma. Over the years, there has been controversy about the relationship between EGFR protein expression and clinical characteristics such as tumor growth rate, degree of histological differentiation, lymph node metastasis, and prognosis of patients (Jayaseelan et al., 2013; Sujitha and Kannan, 2013; Annadhasan et al., 2014). Accordingly, EGFR is an important tumor marker. Considering that the overexpression of EGFR in many tumors is closely related to the progression and prognosis of many tumors, therapy targeting EGFR and mutants is of great concern. A large number of studies have shown that EGFR can be used as a target for treating cancers, especially those with high EGFR expressions (Singh et al., 2013; Li et al., 2014).

Laryngeal cancer is a common malignant tumor of the upper respiratory tract, with an incidence of about 25% of that of head and neck cancer. To date, there remain no effective therapies for this cancer. Most studies have reported that EGFR is highly expressed in laryngeal squamous cell carcinoma, but only mildly expressed in vocal cord polyps. Therefore, the clinical prognosis of laryngeal cancer can be determined through detecting the level of EGFR protein. The high expression of EGFR in laryngeal squamous cell carcinoma suggests that it may be a potential therapy target. In the present study, western blot showed that EGFR had significantly higher expressions in HEP-2 cells and laryngeal cancer tissue than in paracancerous tissue and normal laryngeal tissue ($P < 0.05$). On this basis, we constructed an in vitro model of targeted aggregation of GNRs in laryngeal carcinoma cells

to induce cell death by photothermal therapy. MTT assay was used to detect the effects of different concentrations of GNRs and anti-EGFR mAb/GNRs on cell viability. GNRs and anti-EGFR mAb/GNRs inhibited the survival of HEP-2 cells and BEAS-2B cells, and the effects were augmented with rising dose. In addition, the cytotoxicity of anti-EGFR mAb/GNRs against HEP-2 cells was higher than that of GNRs, whereas its cytotoxicity against normal BEAS-2B cells was lower. Hence, the toxicity of GNRs after antibody binding was much smaller than that of GNRs themselves, further proving that the binding of GNRs to anti-EGFR mAb greatly reduced its cytotoxicity and improved its biocompatibility. The results herein are consistent with those of previous studies on gold nanoparticles (Qu and Lü, 2009; Basavegowda et al., 2014; Zhang et al., 2014). In the present study, through functional modification, GNRs specifically bound EGFR on the surface of cancer cell membrane after binding its antibody. Under NIR irradiation, GNRs efficiently absorbed light energy and converted it into heat, and so the growth of tumor cells was significantly inhibited, even leading to death. Regardless of using GNRs or anti-EGFR mAb/GNRs, the inhibitory effects of NIR irradiation at the same power on the growth of HEP-2 cells surpassed those on BEAS-2 cells, indicating that tumor cells were more sensitive to heat than normal cells, like those reported previously (Azizi et al., 2014; Vijayan et al., 2014; Anand et al., 2015). In other words, irradiating tumors using GNRs indeed had considerable effects (Huang et al., 2006; Chen et al., 2016). In addition, we found that the survival rate of HEP-2 cells in the anti-EGFR mAb/GNRs group was significantly lower than that of the GNRs group ($P < 0.05$), suggesting that GNRs

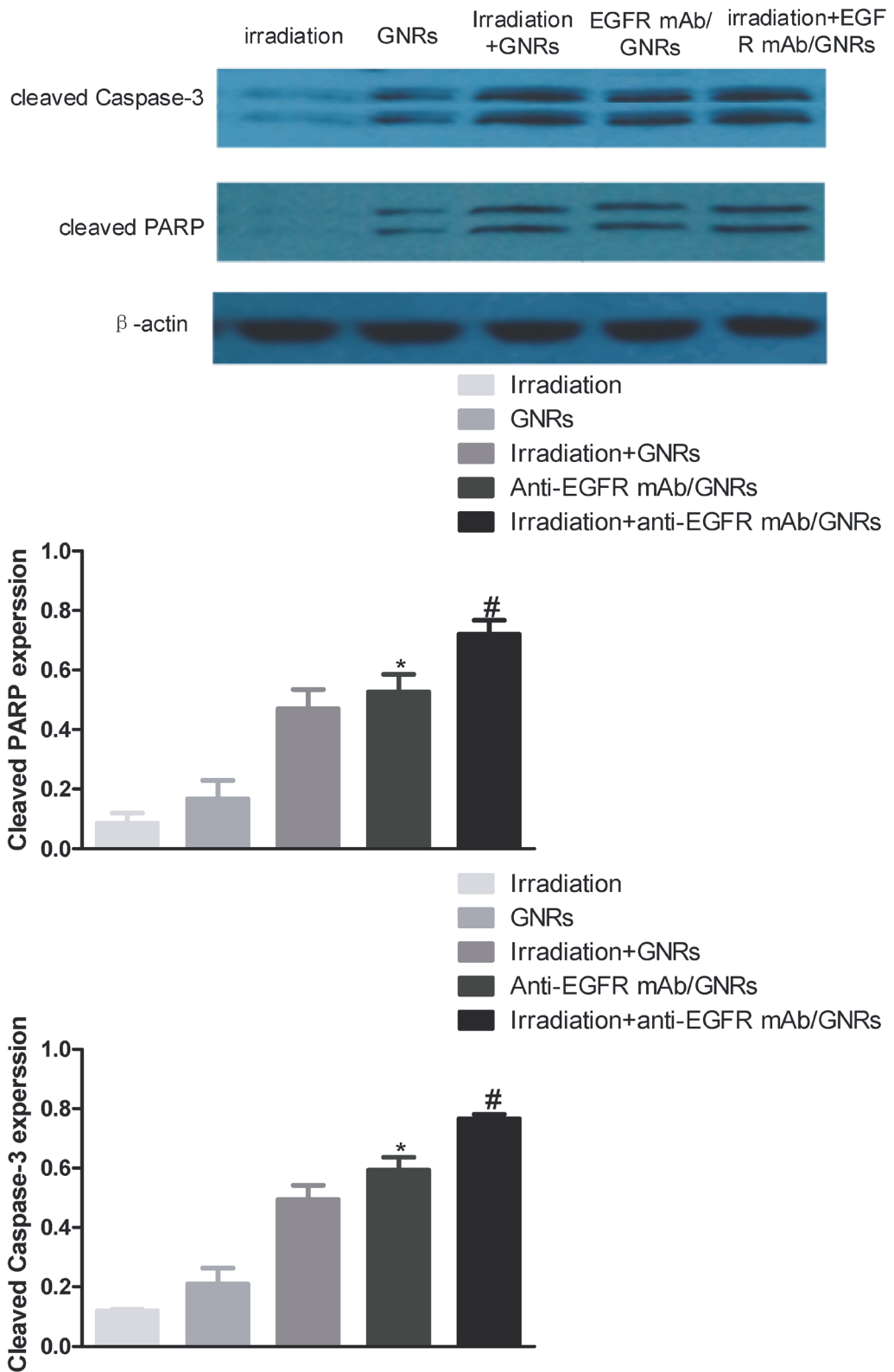


Figure 6. Cleaved PARP and cleaved caspase-3 expressions detected by western blot. *Comparison between anti-EGFR mAb/GNRs group and GNRs group, $P < 0.05$; #comparison between irradiation + anti-EGFR mAb/GNRs group and irradiation + GNRs group, $P < 0.05$.

became targeting after binding antibody and that EGFR targeted HEP-2 cells.

Tumor thermal therapy heats tissue to a temperature that can kill tumor cells (42–43.5 °C) using physical methods, which is maintained for 60–120 min. Any cell population grows through two ways: increase of number and enlargement of volume. Although they may both occur during the development of organisms, increase of cell number is predominant in most cases, being both normal and abnormal. Therefore, the decrease in cell viability after GNRs treatment can also be caused by cell damage, death, or apoptosis (Du et al., 2014; Paul et al., 2015; Velusamy et al., 2015). In the present study, the apoptosis rate of the anti-EGFR mAb/GNRs group was significantly higher than that of the GNRs group, and the apoptosis rate of the irradiation + anti-EGFR mAb/GNRs group also significantly exceeded that of the irradiation + GNRs group ($P < 0.05$). Thus, obvious apoptosis or death did not occur in the irradiation

group, and the promoting effects of anti-EGFR mAb/GNRs on the apoptosis of HEP-2 cells surpassed those of GNRs.

In summary, GNRs enhanced the targeted specificity to tumor cells by functionalization with EGFR, accompanied by improved biocompatibility and stability. Normal tissue damages resulting from inaccurate location of photosensitizers and heat sensitizers in previous thermal therapies were herein evidently relieved, verifying that anti-EGFR mAb/GNRs have great potential in biomedical fields. Therefore, this study may provide a valuable reference for targeted therapy of laryngeal cancer and other malignancies.

Acknowledgments

This study was financially supported by the National Natural Science Foundation of China (No. 81571806) and Key Project of Science and Technology Commission of Nanjing (No. 201402006).

References

- Anand K, Gengan RM, Phulukdaree A, Chuturgoon A (2015). Agroforestry waste *Moringa oleifera* petals mediated green synthesis of gold nanoparticles and their anti-cancer and catalytic activity. *J Ind Eng Chem* 21: 1105-1111.
- Annadhasan M, Muthukumarasamyvel T, Sankar Babu VR, Rajendiran N (2014). Green synthesized silver and gold nanoparticles for colorimetric detection of Hg^{2+} , Pb^{2+} , and Mn^{2+} in aqueous medium. *ACS Sustain Chem Eng* 2: 887-896.
- Azizi S, Ahmad MB, Namvar F, Mohamad R (2014). Green biosynthesis and characterization of zinc oxide nanoparticles using brown marine macroalga *Sargassum muticum* aqueous extract. *Mater Lett* 116: 275-277.
- Basavegowda N, Idhayadhulla A, Lee YR (2014). Phyto-synthesis of gold nanoparticles using fruit extract of *Hovenia dulcis* and their biological activities. *Ind Crop Prod* 52: 745-751.
- Chen S, Bap C, Zhang C, Yang Y, Wang K, Chikkaveeraiah BV, Wang Z, Huang X, Pan F, Wang K et al. (2016). EGFR antibody conjugated bimetallic Au@Ag nanorods for enhanced SERS-based tumor boundary identification, targeted photoacoustic imaging and photothermal therapy. *Nano Biomed Eng* 8: 315-328.
- Du X, Chen Z, Li Z, Hao H, Zeng Q, Dong C, Yang B (2014). Dip-coated gold nanoparticle electrodes for aqueous-solution-processed large-area solar cells. *Adv Energy Mater* 4. doi: 10.1002/aenm.201400135.
- Haapaniemi A, Kankaanranta L, Saat R, Koivunoro H, Saarilahti K, Mäkitie A, Atula T, Joensuu H (2016). Boron neutron capture therapy in the treatment of recurrent laryngeal cancer. *Int J Radiat Oncol Biol Phys* 95: 404-410.
- Huang X, El-Sayed IH, Qian W, El-Sayed MA (2006). Cancer cell imaging and photothermal therapy in the near-infrared region by using gold nanorods. *J Am Chem Soc* 128: 2115-2120.
- Jayaseelan C, Ramkumar R, Rahuman AA, Perumal P (2013). Green synthesis of gold nanoparticles using seed aqueous extract of *Abelmoschus esculentus* and its antifungal activity. *Ind Crop Prod* 45: 423-429.
- Li N, Zhao P, Astruc D (2014). Anisotropic gold nanoparticles: synthesis, properties, applications, and toxicity. *Angew Chem Int Edit* 53: 1756-1789.
- Misono S, Marmor S, Yueh B, Virnig BA (2014). Treatment and survival in 10,429 patients with localized laryngeal cancer: a population-based analysis. *Cancer* 120: 1810-1817.
- Paul B, Bhuyan B, Purkayastha DD, Dey M, Dhar SS (2015). Green synthesis of gold nanoparticles using *Pogestemon benghalensis* (B) O. Ktz. leaf extract and studies of their photocatalytic activity in degradation of methylene blue. *Mater Lett* 148: 37-40.
- Qu Y, Lü X (2009). Aqueous synthesis of gold nanoparticles and their cytotoxicity in human dermal fibroblasts–fetal. *Biomed Mater* 4: 025007.
- Singh M, Kalaivani R, Manikandan S, Sangeetha N, Kumaraguru AK (2013). Facile green synthesis of variable metallic gold nanoparticle using *Padina gymnospora*, a brown marine macroalga. *Appl Nanosci* 3: 145-151.
- Sujitha MV, Kannan S (2013). Green synthesis of gold nanoparticles using *Citrus* fruits (*Citrus limon*, *Citrus reticulata* and *Citrus sinensis*) aqueous extract and its characterization. *Spectrochim Acta A Mol Biomol Spectrosc* 102: 15-23.

- Suman TY, Rajasree SRR, Ramkumar R, Rajthilak C, Perumal P (2014). The green synthesis of gold nanoparticles using an aqueous root extract of *Morinda citrifolia* L. Spectrochim Acta A Mol Biomol Spectrosc 118: 11-16.
- Velusamy P, Das J, Pachaiappan R, Vaseeharan B, Pandian K (2015). Greener approach for synthesis of antibacterial silver nanoparticles using aqueous solution of neem gum (*Azadirachta indica* L.). Ind Crop Prod 66: 103-109.
- Vijayan SR, Santhiyagu P, Singamuthu M, Kumari Ahila N, Jayaraman R, Ethiraj K (2014). Synthesis and characterization of silver and gold nanoparticles using aqueous extract of seaweed, *Turbinaria conoides*, and their antimicrofouling activity. Sci World J 2014: 938272.
- Wolf GT, Bellile E, Eisbruch A, Urba S, Bradford CR, Peterson L, Prince ME, Teknos TN, Chepeha DB, Hogikyan ND et al. (2017). Survival rates using individualized bioselection treatment methods in patients with advanced laryngeal cancer. JAMA Otolaryngol Head Neck Surg 143: 355-366.
- Zahoor T, Dawson R, Sen M, Makura Z (2017). Transoral laser resection or radiotherapy? Patient choice in the treatment of early laryngeal cancer: a prospective observational cohort study. J Laryngol Otol 131: 541-545.
- Zhang S, Li Y, He X, Dong S, Huang Y, Li X, Li Y, Jin C, Zhang Y, Wang Y (2014). Photothermalysis mediated by gold nanorods modified with EGFR monoclonal antibody induces Hep-2 cells apoptosis in vitro and in vivo. Int J Nanomed 9: 1931-1946.
- Zhong Y, Peng F, Bao F, Wang S, Ji X, Yang L, Su Y, Lee ST, He Y (2013). Large-scale aqueous synthesis of fluorescent and biocompatible silicon nanoparticles and their use as highly photostable biological probes. J Am Chem Soc 135: 8350-8356.